REMARKS

This amendment is in response to the final office action dated December 24, 2008. Claims 1-28 are pending and rejected. Claims 1-4, 6-11, 14-18, 20-26, and 28 were rejected as obvious in view of the combination of U.S. Patent No. 6,172,483 to Champlin et al. ("Champlin") and U.S. Patent No. 6,094,033 to Ding et al. ("Ding"). The applicants respectfully traverse the allegations and respond as follows.

CLAIMS 1-28 MEET THE REQUIREMENTS OF SECTION 103(a)

The issue of patentability raised by the final office action, and which the applicants must overcome, is whether each and every limitation of claims 1-28 is found in the relied upon references, and whether the combinations render unpatentable the claims under 35 U.S.C. §103(a). The applicants submit that claims 1-28 meet the requirements of 35 U.S.C. §103(a), and therefore, claims 1-28 are allowable. Applicants address the rejections separately as to each independent claim and the claims that depend therefrom.

1. Claims 1-13

Independent claim 1 is directed to a method for determining a state-of-charge of a battery that includes evaluating a transition frequency of an impedance for a battery, which is excited by an alternating current, and assigning the transition frequency to the state-of-charge of the battery wherein the transition frequency is a frequency of the alternating current at which the imaginary part of the impedance of the battery vanishes. Applicants respectfully assert that this recited method for determining a state of charge of a battery is fundamentally different from the methods disclosed in the relied upon references.

Champlin generally discloses a method for determining the real and the imaginary part of the impedance of a battery (*see, for example,* col. 2, ll. 1-7 of Champlin). Ding generally discloses a battery state-of-charge detector, which can be used to control the charging of a battery (*cf.* col. 2, ll. 54-58), which is related to the battery's impedance, and is determined based on the battery's response at various frequencies. This information is then used to determine the

state-of-charge of the battery (*cf.* col. 5, ll. 6-64). Specifically, the battery's internal resistance is measured and associated with the state-of-charge (*cf.* col. 6, ll. 23-32).

In contrast thereto, the invention recited in pending claim 1 recites determining the state-of-charge of a battery using the transition frequency of the battery, which is the frequency at which the imaginary part of the impedance vanishes.

It is respectfully submitted that the battery's internal resistance and the transition frequency are fundamentally different parameters of the battery. Although both parameters are related to the intersection point between the impedance spectrum and the real axis, they are independent from each other and they are different in their origin, their behavior and their utility. This has already been described in the response to the first office action and will not be repeated again for the sake of brevity. In addition, the difference between the internal resistance and the transition frequency of a battery will be discussed in more detail below.

The first parameter, which can be derived from this intersection point between the impedance spectrum and the real axis, is the value of the ohmic resistance (R) that corresponds to the real part of the battery's impedance. An average value for a lead-acid battery is approximately 5 $m\Omega$. The components responsible for the ohmic resistance are basically the electrolyte/separator, the grids and the pole of the battery. The ohmic resistance is independent of capacitive and faradic electrochemical processes at the electrode/electrolyte interface of the battery. The correlation between ohmic resistance and state-of-charge is based on an increase of the ohmic resistance upon battery discharge. In the specific case of a lead-acid system, this is due to a consumption of electrolyte during discharge (and, as it is known by one of ordinary skill in the art, a decrease in the electrolyte concentration increases the resistance). In this case, the impedance diagrams move in a horizontal direction from the left-hand side to the right-hand side, thereby increasing the internal resistance when state-of-charge decreases. If a different battery system such as a Ni-MH or a Ni-Cd system is considered, in which the overall electrolyte concentration remains unchanged upon discharge, the battery's resistance exhibits miniscule (hardly measurable) and un-exploitable variations (*see* paragraph [0008] of the specification). This phenomenon is known and is consistent with the article *Monitoring State-of-Charge of Ni-MH and Ni-Cd Batteries Using Impedance Spectroscopy*, by A. Hammouche et al., J. Power Sources, 127 (2004) 105-111, Figures 4 and 9 (attached hereto as Exhibit A).

A different parameter, which is related to the intersection point between the impedance spectrum and the real axis, is the transition frequency. The transition frequency is based on the shift of the impedance spectrum in the vertical direction (Frequency distribution). Actually, in the region of the impedance diagram between ca. 5000 and 10 Hz the imaginary part of the impedance diagram measures a mixed "inductive/capacitive" behavior due to the electrochemical processes at the electrode/electrolyte interface. In the higher frequency part of this domain (at ca. 5000-1000Hz), the inductive behavior dominates (therefore the overall imaginary impedance is positive) and in the lower frequency part of this domain (at ca. 100-10Hz), the capacitive behavior dominates (therefore the overall imaginary impedance is negative), and there is a single frequency in between, where the inductive impedance and the capacitive impedance are equal and compensate for each other. The overall imaginary part of the impedance is zero at this special frequency, which is the transition frequency.

When the state-of-charge decreases, the inductive impedance imaginary part remains almost constant while the capacitive impedance imaginary part increases due to the decrease of the plate active surface area, which pulls the whole diagram in the vertical direction. The overall impedance imaginary part becomes equal to zero at another value of the transition frequency. It was the inventors of the present application that found that there is a clear-cut correlation between transition frequency and a battery's state-of-charge. This correlation is used in the method recited in pending claim 1 to determine the state-of-charge of a battery.

As described previously, the transition frequency (related to the capacitive/inductive behavior of the electrodes) has nothing to do with the internal resistance of the battery, which is related to the ohmic resistance of the electrolyte and the grids, expect the fact that, by coincidence, the two parameters relate to the same point on the impedance spectrum.

The study (article attached) that the authors performed on alkaline batteries, where the resistance hardly varies with the state-of-charge, shows that the impedance diagrams hardly move in the horizontal direction (Figures 1 and 6), but do move in the vertical direction ($f_{\pm}$ in Figures 5 and 10). This effectively proves that it concerns two distinct parameters. Furthermore, it should be noted that, to the best of the inventors' knowledge, the approach based on the transition frequency is the only method to track the state-of-charge in sealed alkaline Ni-MH batteries.

As a consequence of the fact that the battery's internal resistance and transition frequency are fundamentally different parameters of a battery, independent claim 1, and claims 2-13 dependent thereon, are inventively distinguished over of the applied prior art.

It is further alleged on page 3 of the Office action that "it would have been obvious to one of ordinary skill in the art at the time the invention was made to have had the teachings of Ding in the device of Champlin to have had obtained SOC based on the batteries [*sic*] internal resistance." However, no other explanation or reasoning is given as to why it would have been obvious to combine the references. It is axiomatic that the analysis provided when rejecting a claim based on obviousness should be made explicit to facilitate review. *KSR*, 127 S.Ct. at 1740-41, 82 USPQ2d at 1396. (*citing In re Kahn*, 441 F.3d 977, 988, 78 USPQ2d 1329, 1336 (Fed. Cir. 2006) ("Rejections on obviousness grounds cannot be sustained by mere conclusory statements; instead, there must be some articulated reasoning with some rational underpinning to support the legal conclusions of obviousness")).

> A factfinder should be aware, of course, of the distortion caused by hindsight bias and must be cautious of arguments reliant upon *ex post* reasoning. See *Graham* 383 U.S. at 36, 86 S.Ct. 684 (warning against a "temptation to read into the prior art the teachings of the invention in issue" and instructing courts to "'guard against slipping into the use of hindsight'" (quoting *Monroe Auto Equipment C. v. Heckethorn Mfg. & Supply Co.*, 332 F.2d 406, 412 (C.A.6 1964))).

KSR, 127 S.Ct. at 1742, 82 USPQ2d at 1397.

Moreover, Applicants respectfully submit that one of ordinary skill in the art at the time of the invention would not have looked to combine Ding with Champlin because Ding is directed completely to measuring a battery's internal resistance. Because of this focus by Ding to measure the battery's internal resistance, one of ordinary skill in the art would not have looked to combine these references. Such a combination would result in a system that still would not have the functionality of that provided by the invention recited in pending claim 1. It is error to reconstruct the patentee's claimed invention from the prior art by using the patentee's claims as a "blueprint." When prior art references require selective combination to render obvious a subsequent invention, there must be some reason for the combination other than the hindsight obtained from the invention itself. *Interconnect Planning Corp. v. Feil*, 774 F.2d 1132, 227 USPQ 543 (Fed. Cir. 1985). Because of Ding's focus on internal battery resistance – there

would have been no motivation to one of ordinary skill in the art to modify the teachings of the cited references to combine certain elements from Ding with the teachings from Champlin. While it may appear obvious in hindsight to make the combination, applicants see no reason from the prior art relied upon by the Examiner why one having ordinary skill in the art would have made the combination absent the applicants' teaching to do so. Thus, a *prima facie* case of obviousness does not exist, and claim 1, and claims 2-13 dependent thereon, are in condition for allowance.

2. Claims 14-28

Independent claim 14 recites a device for determining a state-of-charge of a battery, comprising an element for determining a transition frequency of an impedance of a battery, which is excited by an alternating current, and a calculation unit for assigning the transition frequency to the state-of-charge of the battery, where the transition frequency is a frequency of the alternating current at which the imaginary part of the impedance of the battery vanishes.

In particular, claim 14 recites limitations similar to limitations found in claim 1. Claim 14, and claim 15-28 dependent thereon, are thus allowable for the reasons discussed above.

Conclusion

In view of the foregoing, it is respectfully submitted that the above application is in condition for allowance, and reconsideration is respectfully requested. If there is any matter that the Examiner would like to discuss, the Examiner is invited to contact the undersigned representative at the telephone number set forth below. In any event, the Director is hereby authorized to charge any deficiency in the fees filed, asserted to be filed or which should have been filed herewith to our Deposit Account No. 13-2855, under Order No. 30882/41934.

Date: February 24, 2009

Respectfully submitted,

By /Randall G. Rueth/ 45,887
Randall G. Rueth, Reg. No. 45,887
MARSHALL, GERSTEIN & BORUN LLP
233 S. Wacker Drive, Suite 6300
Sears Tower
Chicago, Illinois 60606-6357
Attorney for Applicant

Available online at www.sciencedirect.com
SCIENCE DIRECT®
Journal of Power Sources 127 (2004) 105–111
JOURNAL OF POWER SOURCES
www.elsevier.com/locate/jpowsour

Monitoring state-of-charge of Ni–MH and Ni–Cd batteries using impedance spectroscopy

Abderrezak Hammouche*, Eckhard Karden, Rik W. De Doncker

Institute for Power Electronics and Electrical Drives, Aachen University of Technology, Jägerstrasse 17–19, D-52066 Aachen, Germany

Abstract

This paper reports on laboratory studies into the ac impedance spectra of nickel–metal hydride and nickel–cadmium batteries, aiming at finding out possible correlation between electrical parameters, extracted directly from the high frequency region, and the battery state-of-charge (SoC). Impedance diagrams were recorded immediately after interrupting the dc charge, or discharge, current. The study revealed that the series resonance frequency, at which the dynamic cell behavior switches from an inductive character ($Z'' > 0$) to a capacitive one ($Z'' < 0$), varied monotonously as a function of state-of-charge. This behavior was reproducible after intermittent charge and discharge. Half-cell measurements were also conducted to associate the cell impedance with either processes occurring at the positive or negative plates.

Keywords: Ni–MH; Ni–Cd; Battery state-of-charge; Impedance spectroscopy; Series resonance frequency

1. Introduction

Sealed nickel–metal hydride and nickel–cadmium secondary batteries, have demonstrated a rapid expansion in many areas of battery usage. For practical purposes, a technique capable of predicting the residual capacity with sufficient accuracy is urgently required. This applies particularly to the new 42 V-system where the battery is strained to a state-of-charge (SoC) as low as 40%. Traditional solutions used for vented lead–acid cells, such as specific gravity or electrolyte resistance measurements, cannot be applied to these sealed systems because the cell electrolyte composition remains virtually constant during charge–discharge cycles. The only reliable procedure to determine battery SoC and aging effects is to perform a complete discharge–charge cycle. This operation is obviously expensive, time-consuming and leaves the batteries to be tested out of service during the testing time.

Impedance spectroscopy is used to make a fast, non-destructive and reliable method for such a characterization. The objective consists of inferring from the impedance spectra, plotted in different conditions, one or many electrical parameters, which increase or decrease monotonically as a function of the battery SoC. Such parameters should be: (i) simple to measure; (ii) reproducible; and (iii) quickly accessible.

Research in laboratories on impedance parameters related to state-of-charge or state-of-health of battery cells has been carried out over the last two decades [1–4]. Hampson et al. [5], Huet [6] and Rodrigues et al. [7] reviewed the published data on impedance studies of batteries and battery electrodes, undertaken for this purpose. It has been shown that various parameters may be useful to estimate the status of battery systems under different experimental conditions (under load or at open circuit after a period of rest), particularly of lead–acid and nickel–cadmium secondary batteries, but little thorough work on impedance parameters related to Ni–MH batteries has been done so far [8].

Earlier measurements conducted on alkaline batteries [2,3,9,10], investigating cell response in the high frequency domain, were not conclusive because the electrolyte does not participate to the overall electrode processes, whereas a pronounced effect of SoC was observed on those electrical quantities extracted from the low frequency region of the impedance diagrams, such as the impedance modulus, the phase angle, the equivalent series and parallel capacitance of the cell. However, it should be noted that measurements at low frequencies are time-consuming and, hence, less suitable for routine monitoring of cells in service.

Besides, most of these studies were concerned with small capacity batteries, typically less than 10 Ah. Such cells generally present impedance magnitudes ranging from some

* Corresponding author. Tel.: +49-241-80-96973; fax: +49-241-80-92203.
E-mail address: hm@isea.rwth-aachen.de (A. Hammouche).

0378-7753/$ – see front matter © 2003 Elsevier B.V. All rights reserved.
doi:10.1016/j.jpowsour.2003.09.012

tens of milliohm up to several ohms, depending on the measuring frequency and SoC. Several commercial impedance meters exist in the market which enable experimental measurement of such impedances. However, for larger capacity batteries, the impedance magnitude falls well below the milliohm range. As a result, more precise and reliable instrumentation is needed [11].

The aim of the present study is to scrutinize the high frequency region of the cell impedance spectra in order to evince possible relationship between high frequency electrical parameters and SoC. The investigation was undertaken on two kinds of rechargeable alkaline batteries: Ni–MH and Ni–Cd systems with relatively large capacity, using dedicated high-precision instrumentation.

2. Experimental

Measurements were carried out on vented Ni–Cd batteries manufactured by Hoppecke under the reference name FNC-T 204H, with a nominal capacity of 46 Ah cells. The cells were first conditioned at room temperature for a few cycles, using a Digatron test facility, to stabilize their discharge capacity. They were cycled by charging first at *C*/2 rate to reach 60% SoC and further at *C*/10 rate to achieve a total overcharge factor of 1.4. After a rest for 5 min, the cells were discharged at *C*/5 rate to a cut-off voltage of 1.0 V.

Sealed prismatic Ni–MH cells with a rated capacity of 42 Ah (Varta NP 42) were also studied. They were cycled, as specified by the manufacturer, by charging at *C* rate to reach 80% *C*, resting for 5 min and followed by further charging 30% of the nominal capacity at *C*/5 rate. The discharge operation was made with a *C* rate to a cut-off voltage of 1.0 V.

Impedance measurements were conducted at various states of charge, stepped with approximately 10% SoC, on open circuit, immediately after charge or after discharge. Starting at the fully discharged state, the cells were charged intermittently at *C*/5 rate for 1/2 h to achieve increasing SoCs. They were systematically discharged at *C*/5 down to 1.0 V after plotting the impedance spectra, to determine their actual state-of-charge, before recharging to the next SoC. Impedance spectra were also recorded at different SoCs immediately after intermittent discharges.

Laboratory instrumentation, used for the present experiments, has been developed at ISEA for high-precision impedance measurements on industrial batteries [12]. In order to ensure that impedance measurements are performed under linear conditions, the ac current amplitude was automatically chosen for each frequency so that the maximum ac voltage response was equal to 3 mV. In such conditions, the variation in SoC induced by the ac signal during impedance measurements, does not exceed 0.03% for the lowest frequency used. The frequency domain investigated ranged from 3 kHz down to 0.1 Hz, occasionally to 0.01 Hz, with a frequency distribution of 24 frequencies/decade.

Great care has been taken for measuring the low impedances of the cells. The significant contribution of the connecting leads to the measured impedance has been eliminated by using four leads; two for the current flow and the other two for the voltage measurement.

For half-cell measurements, to separately estimate each electrode polarization and impedance for the vented Ni–Cd cell, a mercury/mercurous oxide reference electrode (RE), of standard design, in the same potassium hydroxide concentration as the cell electrolyte, was employed. The RE tip was located in the midpoint of the free liquid electrolyte above the plates, between the two current collecting tabs. In the case of sealed Ni–MH batteries, certain impedance measurements have been performed using the cell case as a reference electrode, as was suggested by Reid [13] for impedance studies of sealed Ni–Cd cells. The voltage of the case with respect to the anode or cathode is unimportant provided that it remains stable during the measurement of the impedance. We checked systematically that the sum of the electrodes potential and impedance match exactly the corresponding cell quantities.

All ac impedance spectra reported in this paper were obtained at laboratory room temperature of 25 ± 1 °C.

3. Results and discussion

In previous studies, the cell impedance was measured in two distinct conditions: either during current flow [2,8,14], or at zero dc current after many hours of rest at open circuit [3,4,8]. The experimental data were then analyzed in light of models to derive useful fitting parameters. In the former case, the system is not in the steady-state conditions (i.e., the state-of-charge continuously drifts, especially during low frequency measurement), which complicates system modeling. The latter case could, however, be reasonably applied only to applications where time is not critical.

In the present experiments, we propose, for practical purposes, to exploit the raw data recorded immediately after interrupting the dc charge or discharge current. Furthermore, data obtained from the high frequency domain is used to derive electrical quantities at specific frequencies or from a narrow frequency interval.

3.1. Nickel–cadmium batteries

Fig. 1 shows the Nyquist loci for Ni–Cd cell at different SoCs, plotted after intermittent charge steps. The shape of the diagrams is basically the same, allowing to perform a unique exploitation of the data. At high frequencies, it displays a pronounced inductive effect. A semi-circle with a depressed shape appears at mid-frequencies, and prolonged by a low frequency tail. The intercept of the spectra with the real axis is labeled R_Ω. This term corresponds to the sum of the ohmic resistances of the electrolyte in the separator, the

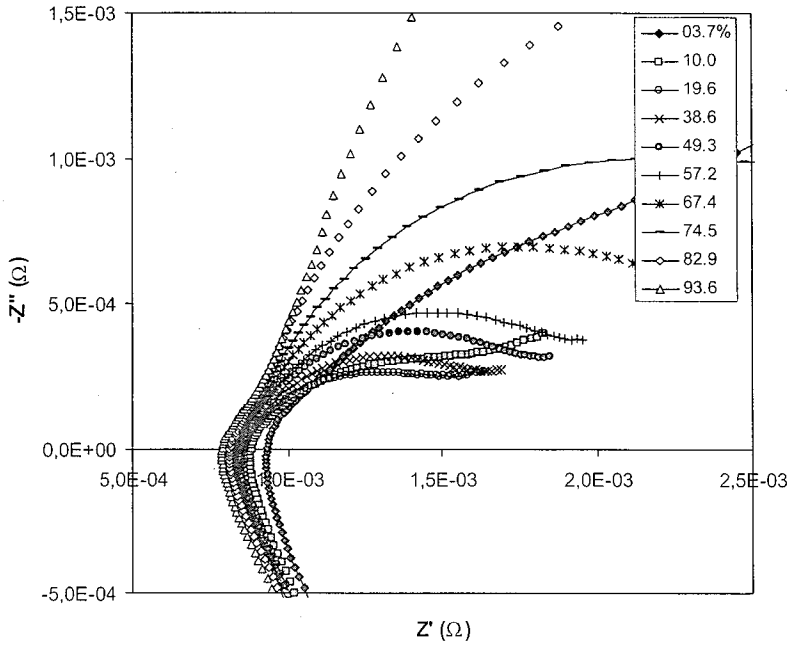

Fig. 1. Impedance spectra of 46 Ah Ni–Cd battery at different SoCs.

electrode active materials, the surface coverage of the electrodes by reaction products, and the connections inside the cell.

The size of the impedance diagram does not change monotonically with SoC: it decreases from a relatively large value at fully discharged state, passing through a minimum at 20% SoC and re-increasing for the higher SoC values.

In order to help determine which electrode is responsible for loss of cell performance, the impedances of positive and negative plates were plotted separately. Their algebraic sum systematically matches the cell impedance (Fig. 2), with the major contribution coming from the negative plates. Xiong et al. [15] arrived at the same conclusion using a galvanostatic non-destructive test method, which consists of recording the variations of the battery voltage, near the cell equilibrium (within 2–3 mV) when applying a very small dc current.

From the general shape of these plots, it appears that the impedance imaginary part, Z'', changes more significantly, in the mid-frequency range, than the corresponding real part. Therefore, for a better resolution, it is more convenient to plot the variations of Z'' than the modulus. Fig. 3 shows the variations of Z'' at fixed frequencies (i.e., 10, 1 and 0.1 Hz). It can be noticed that after a decrease between 0 and 20% SoC, this parameter increases again at higher SoC, pronouncedly at 0.1 Hz.

As mentioned above, parameters that can be extracted from the high frequency domain of the impedance diagrams are preferable. In this respect, we examined the variations of the resistance R_Ω at which the impedance locus crosses the

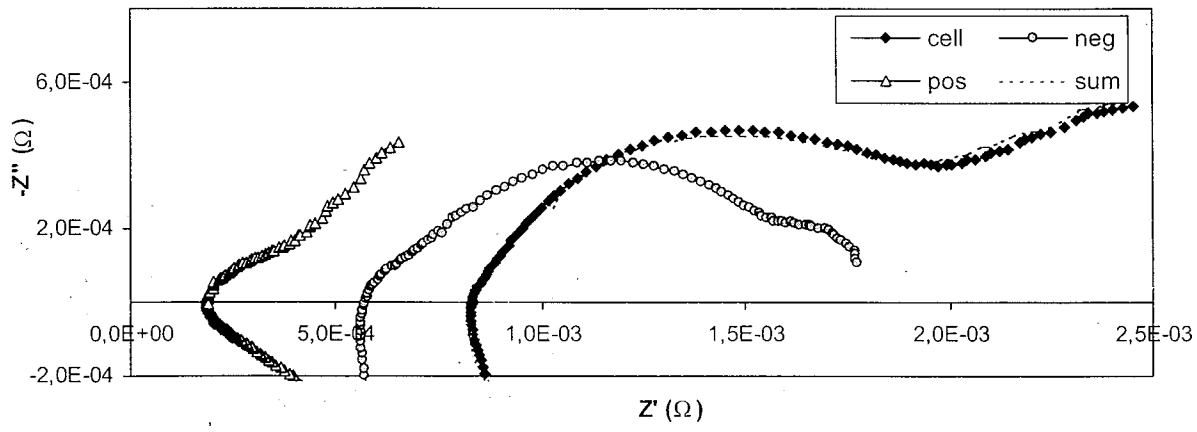

Fig. 2. Typical impedance diagrams of half-cells and complete Ni–Cd cell, at 57% SoC.

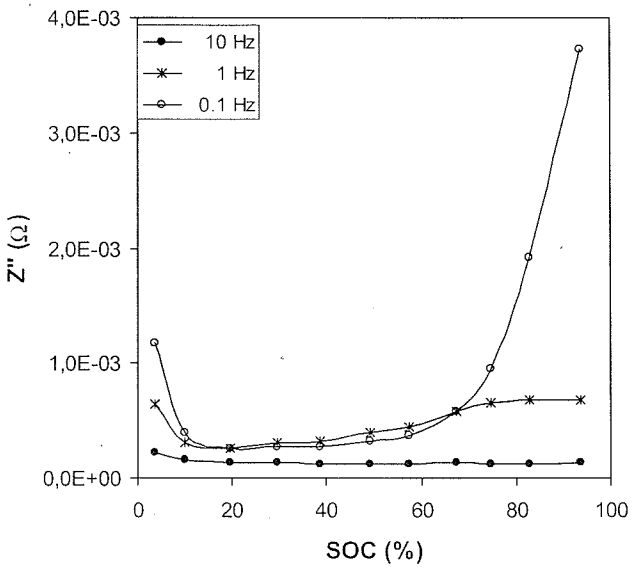

Fig. 3. Variations of the *iso*-frequency imaginary part measured at 10, 1 and 0.1 Hz for Ni–Cd battery.

real axis. Fig. 4 shows that this parameter is hardly usable to accurately estimate SoC due to its minor variations over the 20–100% SoC interval.

Unlike lead–acid batteries, in which the term R_Ω exhibits significant variations due to depletion of H_2SO_4 concentration during discharge, the contribution of the electrolyte in alkaline batteries is expected to be unimportant since KOH concentration remains globally constant during battery operation. This made all former investigations privilege the low frequency domain to deduce SoC indicating parameters. The slight increase observed in R_Ω, on discharge, is likely related with the presence of a substantial amount of poorly conducting $Ni(OH)_2$ at low SoCs [16]. This hypothesis is confirmed by observing an equivalent shift in the R_Ω term on the impedance of the positive plates; the negative plates show no evolution in this parameter.

A second high frequency parameter that can be exploited from the intercept of the spectra with the real axis

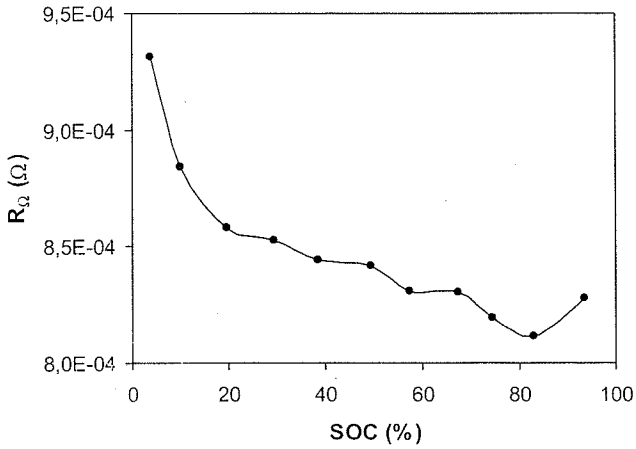

Fig. 4. Evolution of the ohmic resistance with SoC for Ni–Cd battery.

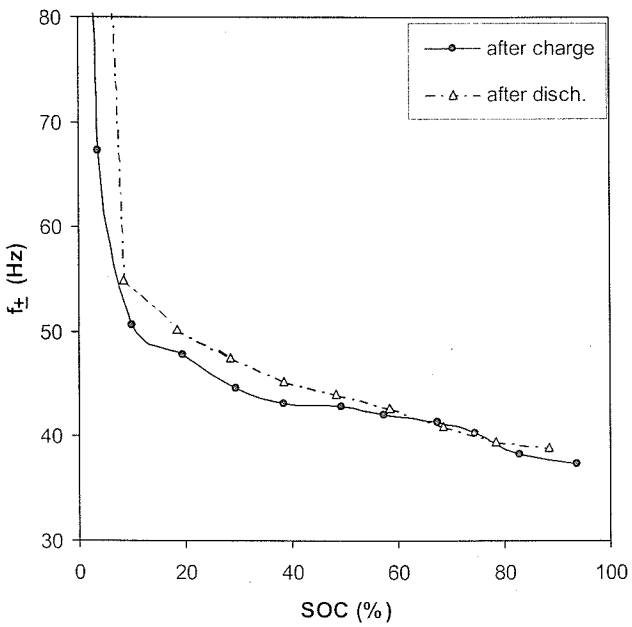

Fig. 5. Series resonance frequency for Ni–Cd battery at different SoCs.

is the frequency at which the impedance passes through series resonance, $f_\pm$, being inductive ($Z'' > 0$) at higher frequencies and capacitive ($Z'' < 0$) at lower frequencies. Determining this parameter, denoted hereafter as $f_\pm$, needs interpolation of this part of the spectrum around the zero imaginary impedance. Fig. 5 shows that $f_\pm$ exhibits monotonous sensitivity to SoC, and so can be used as an indicator for the battery state-of-charge. Interestingly, the figure also shows that the same trend is obtained after intermittent discharges, giving much credibility to $f_\pm$ parameter in inferring battery SoC disregarding the battery operation history.

Unlike previous works, in which the inductive branch was systematically omitted, in the present work, we emphasize the 300–30 Hz frequency region where the inductive behavior is strongly present. In this region, the cell has mixed inductive–capacitive dynamic behavior extending on either side of this transition frequency. The resulting impedance diagram is consequently strongly deformed. This can be better viewed when Z'' is presented as a function of $\log(f)$ showing how steeply the curve intercepts the frequency axis. In the opposite case, where these two behaviors are unambiguously uncoupled, concentrated points are present in the vicinity of $f_\pm$ [17]. Such a mixed (inductive–capacitive) dynamic behavior is a specific feature of electrochemical power sources in view of their low-resistance and large-electrode capacitance. The inductive effect can be minimized by using the 4-contact measuring procedure and by twisting the electrical wires, but cannot be completely suppressed since the cell contains at least part of the leads. The value of the inductance for the present cells amounts to approximately 50 nH, deduced from 500 to 200 Hz interval in which the curve appears quite vertical. For reproducible measurements, the

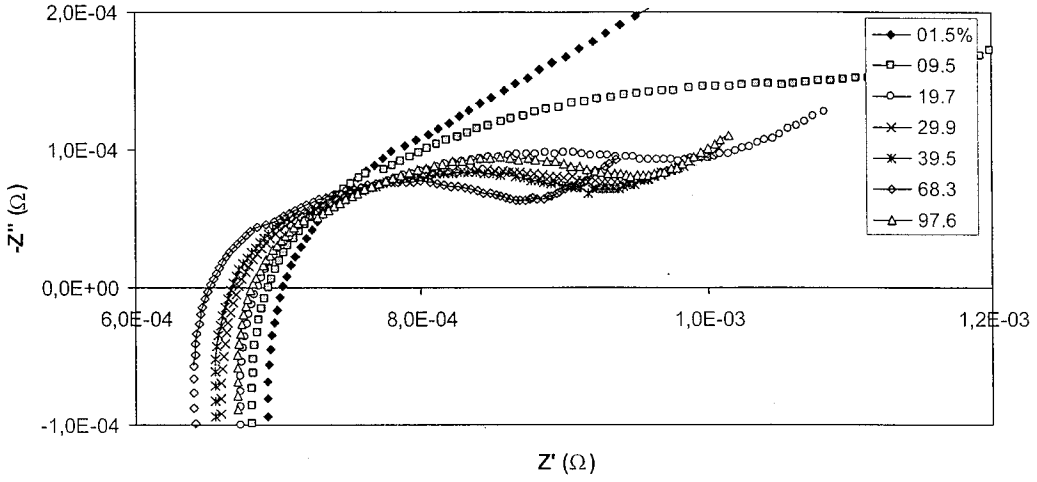

Fig. 6. Impedance spectra of 42 Ah Ni–MH battery at different SoCs.

connections must be built in a well-defined geometrical arrangement.

3.2. Nickel–metal hydride batteries

Fig. 6 shows the Nyquist plots for Ni–MH battery at some SoCs recorded immediately after switching off the dc charge current. The diagrams are composed of a semi-circle-like loop, which changes into a straight line as the frequency decreases. Apparently, while the shape does not change much with SoC, the whole impedance diagram shifts towards lower Z values when SoC increases in the 0–90% range. However, for 100% SoC, the opposite trend is observed, consistently with data on similar cells having a lower capacity [8].

On Fig. 7, the impedance of the positive and negative plates, measured against the cell case, is given. The sum of the half-cell impedance results fits the two-electrode measurement, confirming the validity of the measurement. Careful examination of the plates impedance shows that the variations observed in the cell impedance are induced basically by the evolution of the impedance of the positive plates, which shows variations with SoC parallel to those corresponding to the cell; the impedance of the negative plates does not vary with SoC. The positive electrode impedance is likely related to the presence of nickel hydroxide blocking films, reflected in the linear spike appearing in the low frequency region for both of Ni–Cd and Ni–MH cells (Figs. 2 and 7). The behavior of the negative plates has been reported by Zhang et al. [18], who found the charge-transfer resistance of the MH electrode to be practically independent of its SoC, since this electrode does not undergo any significant structural modification during charge–discharge reactions, as these involve only absorption and desorption of hydrogen atoms in the alloy lattice.

Half-cell measurements show particularly that the re-increase of Z at 100% SoC comes from changes in the behavior of the positive plates during overcharge. Actually, the charge-transfer resistance associated with oxygen evolution during the overcharge process is higher than that corresponding to the main redox couple of the battery [19].

To detect a useful correlation between impedance parameters and battery SoC, we examined the evolution of some electrical parameters as for Ni–Cd batteries. From the general shape of these impedance plots, it can be noticed that the impedance real part, Z', changes more significantly, in the mid-frequency range, than the corresponding imaginary part. Fig. 8 shows that this quantity, measured at three fixed frequencies (i.e., 10, 1 and 0.1 Hz), displays a concave shape, going through a minimum extending between 50 and 95% SoC. Hence, the state-of-charge cannot be determined from the value of real component at a fixed frequency.

The ohmic resistance, R_Ω, decreases slowly upon charge, but re-increases for SoC greater than 80% (Fig. 9). This

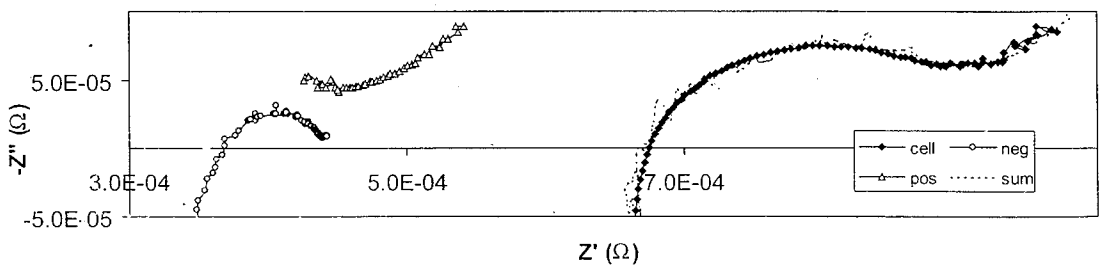

Fig. 7. Typical impedance diagrams of half-cells and complete Ni–MH cell, at 30% SoC.

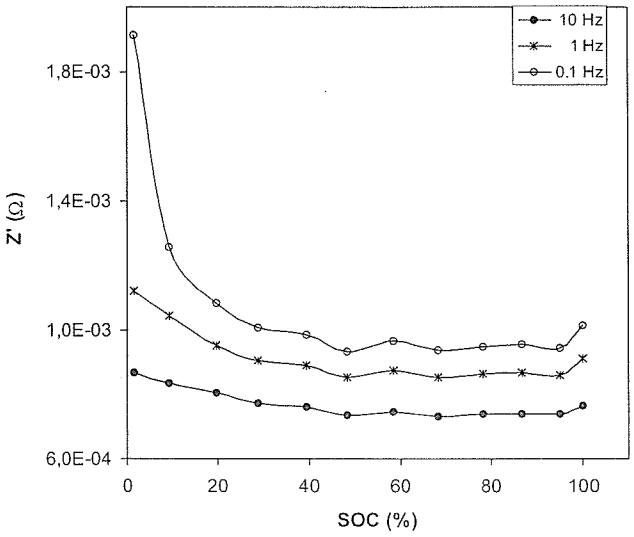

Fig. 8. Variations of the *iso*-frequency real part measured at 10, 1 and 0.1 Hz for Ni–MH battery.

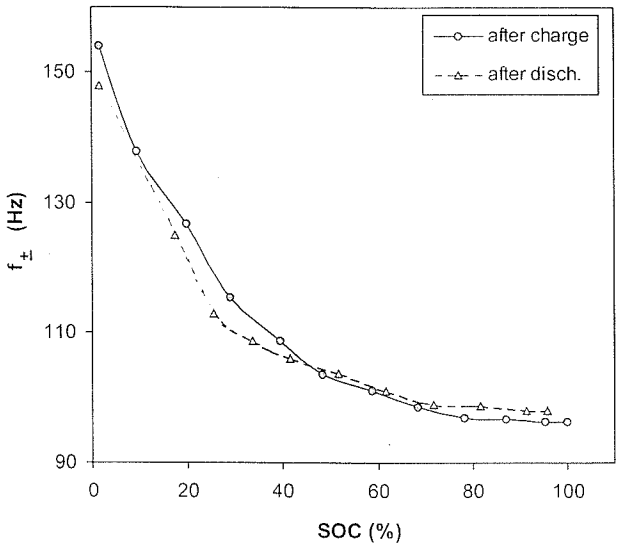

Fig. 10. Series resonance frequency for Ni-H battery at different SoCs.

tendency is similar to what is reported above for Ni–Cd batteries. The positive reaction product, formed upon discharge, and gas dissolution in the electrolyte, produced in the overcharge conditions, are respectively, responsible for the increase of R_Ω at low and high SoC values. Moreover, the small differences measured do not allow accurate determination of SoC from this parameter.

Similar to Ni–Cd batteries, the only parameter that displays monotonous variations with SoC is the series relaxation frequency $f_\pm$ (Fig. 10). It increases continuously from about 95 Hz, for the 100% SoC, up to 150 Hz, for the fully discharged state. Of particular importance, is the reproducibility of $f_\pm$ values recorded upon battery discharge, showing the robustness of such a parameter in inferring the battery SoC irrespective of whether the battery has just been charged, or discharged.

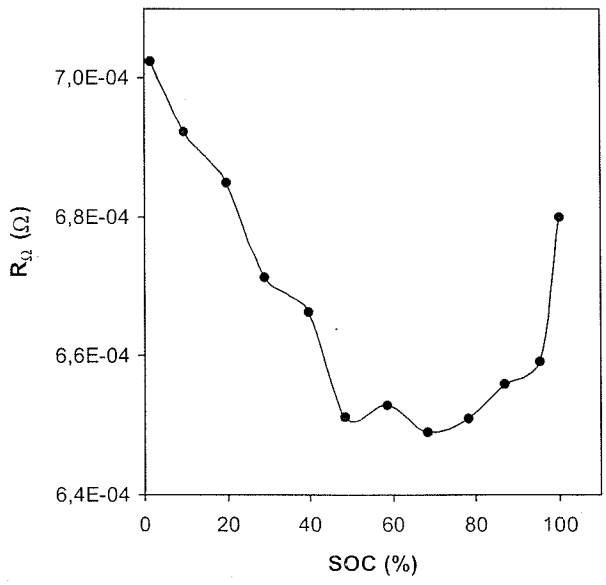

Fig. 9. Evolution of the ohmic resistance with SoC for Ni–MH battery.

4. Conclusions

In this work, we looked for possible correlation between certain electrical parameters derived directly from experimental impedance plots and state-of-charge of rechargeable Ni–MH and Ni–Cd alkaline batteries. Although *iso*-frequency imaginary and real components exhibit significant dependency on SoC, especially at 0.1 Hz, no clear-cut dependency on SoC was found because the variations are not regular to enable unique SoC deduction. The same conclusion is drawn for the ohmic resistance, R_Ω, measured in the high frequency domain.

On the contrary, the series resonance frequency $f_\pm$ exhibits a reproducible monotonous dependency on SoC, either when measured after intermittent charges or discharges. Therefore, it can be concluded that this parameter, which is fast and easy to measure, is effective for routine monitoring the state-of-charge of the tested batteries. This observation must be extended over a wider range of batteries; it does provide strong grounds to pursue ac impedance techniques as probes of state-of-charge of vented and sealed in-service batteries.

Acknowledgements

One of the authors (A.H.) is grateful to the Alexander von Humboldt Foundation for financial support. The authors like to thank Dipl.-Ing. S. Buller, Dipl.-Ing. B. Fricke and Dipl.-Ing. (FH) O. Bohlen for helpful discussions.

References

[1] R.T. Barton, P.J. Mitchell, J. Power Sources 27 (1989) 287.
[2] Ph. Blanchard, J. Appl. Electrochem. 22 (1992) 1121.
[3] V.V. Viswanathan, A.J. Salkind, J.J. Kelley, J.B. Ockerman, J. Appl. Electrochem. 25 (1995) 716.
[4] V.V. Viswanathan, A.J. Salkind, J.J. Kelley, J.B. Ockerman, J. Appl. Electrochem. 25 (1995) 729.
[5] N.A. Hampson, S.A.G.R. Karunathilaka, R. Leek, J. Appl. Electrochem. 10 (1980) 3.
[6] F. Huet, J. Power Sources 70 (1998) 59.
[7] S. Rodrigues, N. Munichandraiah, A.K. Shukla, J. Power Sources 87 (2000) 12.
[8] K. Bundy, M. Karlsson, G. Lindbergh, A. Lundqvist, J. Power Sources 72 (1998) 118.
[9] R. Haak, C. Ogden, D. Tench, J. Power Sources 12 (1984) 289.
[10] M. Hughes, R.T. Barton, S.A.G.R. Karunathilaka, N.A. Hampson, R. Leek, J. Appl. Electrochem. 15 (1985) 129.
[11] R. Heron, M.C. Fadden, J. Dunn, in: Proceedings of the Intellectual Conference, Vancouver, Canada, 1994, p. 270
[12] E. Karden, S. Buller, R.W. De Doncker, J. Power Sources 85 (2000) 72.
[13] M.A. Reid, J. Power Sources 29 (1990) 467.
[14] M. Keddam, Z. Stoynov, H. Takenouti, J. Appl. Electrochem. 7 (1977) 539.
[15] X.Y. Xiong, H. Vander Poorten, M. Crappe, Electrochim. Acta 41 (1996) 1267.
[16] D. Linden, in: D. Linden (Ed.), Handbook of Batteries, Mc-Graw Hill, New York, 1995, pp. 33.1–33.29.
[17] B. Savova-Stoynov, Z.B. Stoynov, J. Appl. Electrochem. 17 (1987) 1150.
[18] W.L. Zhang, M.P.S. Kumar, S. Srinivasan, J. Electrochem. Soc. 142 (1995) 2935.
[19] X. Andrieu, P. Poignat, Power Sources 14 (1995) 43.